

Effect of Fe₂O₃ on Structural and Magnetic Properties of Half Metallic Fe₃O₄ Thin Films

Saira Riaz¹⁾, Usman Khan²⁾, Y.B. Xu³⁾, Shahzad Naseem⁴⁾
and *Attia Awan

^{1), 4)} *Centre of Excellence in Solid State Physics, University of Punjab, Lahore, Pakistan*

²⁾ *IOP, Chinese Academy of Sciences, Beijing, China*

³⁾ *Department of Electronics, University of York, UK*

¹⁾ saira.cssp@pu.edu.pk

ABSTRACT

Ferromagnetic semiconductors are amongst the materials that are promising candidates for spintronic applications because of high-spin polarization. High Curie temperature of the materials is also an extremely crucial requirement for proper functionality of electronic devices. This motivates the scientific community to search for new materials with high Curie temperature as well as high-spin polarization. Among various materials, magnetite (Fe₃O₄) is a promising candidate due to its high Curie temperature and theoretically predicted 100% spin polarization. Magnetite thin films are prepared in this work using sol-gel and spin coating method. Sol concentration is varied as 0.8mM, 1.0mM, 1.2mM, 1.4mM and 1.8mM. XRD patterns indicate formation of magnetite phase at sol concentration 1.8mM. Presence of diffraction peaks corresponding to (421) and (410) indicate the inclusion of Fe₂O₃ phase in Fe₃O₄. With increase in sol concentration the intensity of diffraction peaks corresponding to Fe₂O₃ phase increases. Change of preferred orientation from (400) to (321) plane is observed as sol concentration is decreased to 0.8mM. Films show ferromagnetic behavior and increase in saturation magnetization is observed with decrease in sol concentration to 1.0mM. This indicates that inclusion of Fe₂O₃ phase in Fe₃O₄ leads to increased saturation magnetization while change in preferred orientation at 0.8mM results in decrease in magnetic properties. DFT is used to study half metallic nature of Fe₃O₄.

1. INTRODUCTION

For the last few decades the interest to reduce dimensions of electronic devices and increase their efficiency has tremendously increased. For this purpose, new technologies are being explored worldwide. This thrust of mankind has led us to use additional degree of freedom associated with electron i.e. its spin along with its charge. This will not only scale down the devices but open new doors for future devices (Alraddadi et al. 2016, Bohra et al. 2016, Akbar et al. 2015).

Among the materials that are utilized for various spintronic applications, half metals are considered to be the most important. In half metals the two bands i.e. spin

up and down bands are not symmetric at the Fermi level. In case with 100% spin polarization only one spin band is present at the Fermi level. Metals like iron and cobalt do not have 100% spin asymmetry. Chromium oxide and $\text{La}_{0.7}\text{Sr}_{0.3}\text{MnO}_3$ have 100% spin polarization but their Curie temperature is extremely low. This compelled the scientific community to explore new materials with high spin polarization and high Curie temperature (Gilks et al. 2014, Hevroni et al. 2016). Iron oxide offers the advantages both of high Curie temperature and 100% spin polarization. This material shows conducting nature for one spin orientation and insulating nature for the other spin orientation (Guan et al. 2016, Craik 1975, Gilks et al. 2014, Akbar et al. 2015).

Magnetite (Fe_3O_4 ; $\text{Fe}^{3+}[\text{Fe}^{2+}, \text{Fe}^{3+}]_2\text{O}_4$) possesses cubic inverse spinel structure. It has 8 formula units. There are 24 iron cations (Fe^{3+} and Fe^{2+}) and 32 oxygen anions that are divided in octahedral and tetrahedral sites. Another important form of iron oxide with high magnetization is maghemite ($\gamma\text{-Fe}_2\text{O}_3$). It has the same structure as that of Fe_3O_4 but only Fe^{3+} cations are present. Locations of Fe^{2+} cations are present as vacancies. Magnetization of $\gamma\text{-Fe}_2\text{O}_3$ ($2.5\mu\text{B}$) is less than that of Fe_3O_4 ($4\mu\text{B}$) (Craik 1975, Riaz et al. 2014b).

In the present work, Fe_3O_4 films have been prepared through sol-gel and spin coating process with molar concentration as 0.6mM-1.4mM. Effect of sol concentration on inclusion of $\gamma\text{-Fe}_2\text{O}_3$ phase in Fe_3O_4 and its effect on magnetic properties are investigated in detail.

2. EXPERIMENTAL DETAILS

Preparation of iron oxide thin films was carried out with sol-gel method. $\text{FeCl}_3 \cdot 6\text{H}_2\text{O}$ was used as precursor and deionized water and ethanol were employed as solvents. $\text{FeCl}_3 \cdot 6\text{H}_2\text{O}$ was mixed in deionized (DI) water and ethanol. The solution was then heated at 50°C . Detailed steps for sol synthesis have been reported elsewhere (Riaz et al. 2014a, Akbar et al. 2014a).

For thin film preparation, copper was used as substrate. Etching of copper substrates was done with diluted hydrochloric acid. The substrates were washed with deionized water. These substrates were ultrasonically agitated in acetone and isopropyl for 15 minutes (Asghar et al. 2006a,b). Spin coating of sols was carried out at 3000rpm for 20secs. Films were characterized under as-deposited conditions.

Bruker D8 Advance X-ray diffractometer (XRD) was used for structural analysis. Magnetic properties were studied using Lakeshore's 7407 Vibrating Sample Magnetometer (VSM).

3. RESULTS AND DISCUSSION

X-ray diffraction patterns for iron oxide thin films can be seen in Fig. 1. JCPDS card Nos. 72-2303 and 39-1346 were used for Fe_3O_4 and $\gamma\text{-Fe}_2\text{O}_3$ indexing, respectively. Iron oxide thin films prepared using molar concentration 1.4mM gives Fe_3O_4 phase. The preferred orientation is along (400) plane for Fe_3O_4 phase. With decrease in sol concentration to 1.2mM inclusion from $\gamma\text{-Fe}_2\text{O}_3$ phase was observed indicated by arrows in Fig. 1 but preferred orientation of the films was preserved. As sol concentration was further decreased to 1.0mM and 0.8mM contribution from $\gamma\text{-Fe}_2\text{O}_3$ phase increases. With further decrease in sol concentration to 0.6mM Fe_3O_4 and $\gamma\text{-Fe}_2\text{O}_3$ phases were observed but preferred orientation of the films changed to (321)

plane. Oxidation mechanism that leads to inclusion of maghemite in magnetite is associated with diffusion of iron cations towards the surface and diffusion of oxygen anions to the core of grains. Oxygen ions are larger in radius as compared to iron ions (Jolivet and Tronc 1988, Riaz et al. 2014b) so diffusion of iron cations is much easier in comparison to oxygen ions. Iron cations at the surface react with oxygen anions thus the surface forms $\gamma\text{-Fe}_2\text{O}_3$ like character. At the surface, these iron ions react with oxygen anions and form a thin layer of $\gamma\text{-Fe}_2\text{O}_3$. This results in inclusion of $\gamma\text{-Fe}_2\text{O}_3$ phase in Fe_3O_4 . This transition is associated with less number of iron cations in the unit cell. However, the structure is preserved during this process (Jolivet and Tronc 1988, Riaz et al. 2014b).

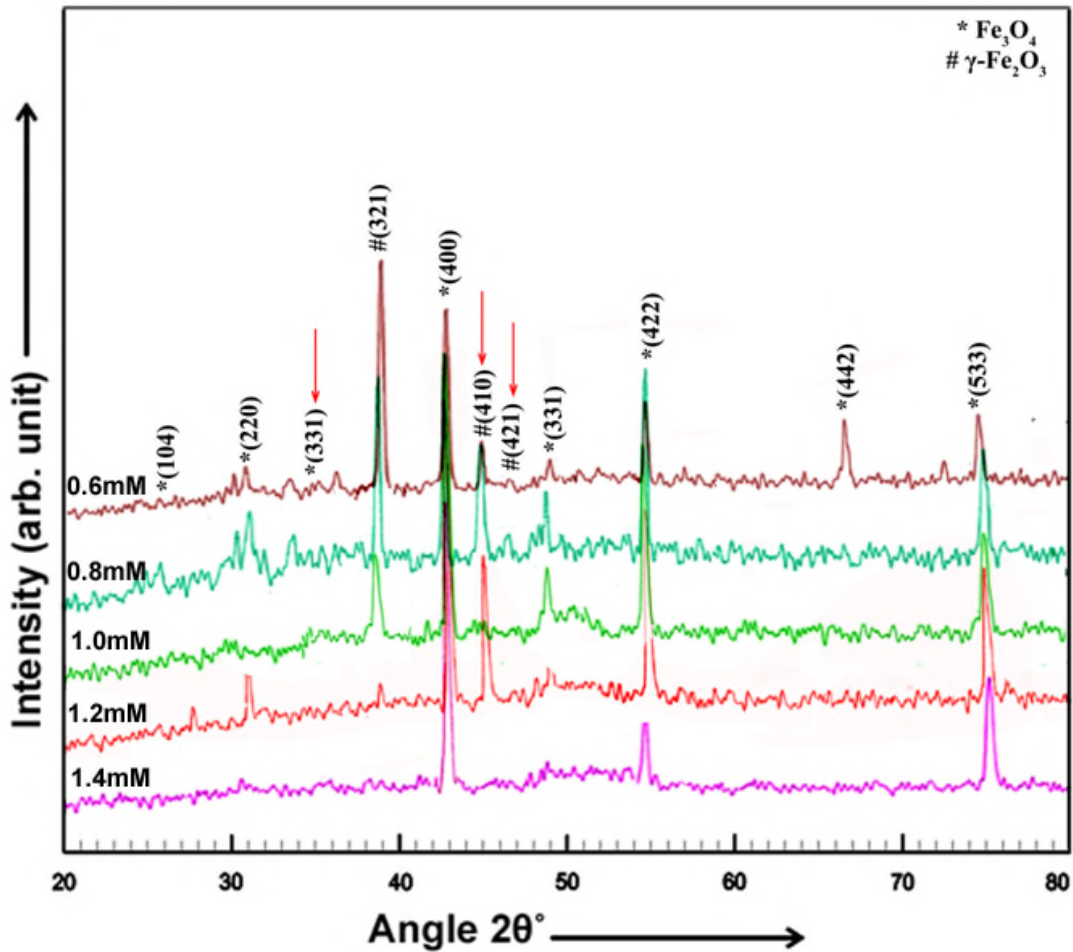


Fig. 1 XRD patterns for iron oxide thin films

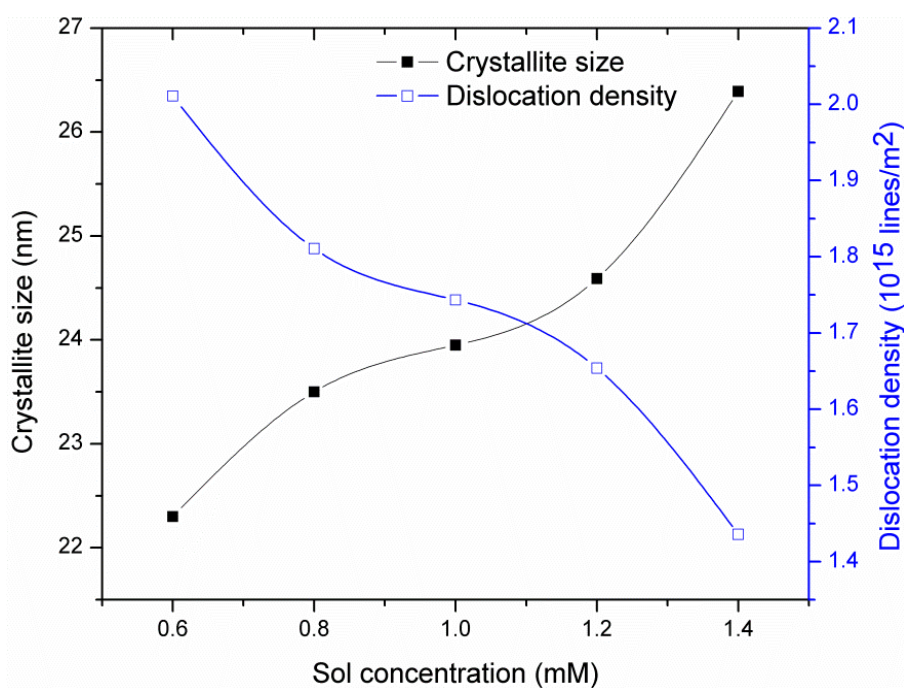
Crystallite size (t), strain (Cullity 1956) and dislocation density (δ) (Kumar et al. 2011) were calculated using Eqs. 1-3.

$$t = \frac{0.9\lambda}{B \cos \theta} \tag{1}$$

$$\delta = \frac{1}{t^2} \tag{2}$$

$$Strain = \frac{\Delta d}{d} = \frac{d_{exp} - d_{hkl}}{d_{hkl}} \quad (3)$$

Where, θ is the diffraction angle, λ is the wavelength (1.5406Å) and B is Full Width at Half Maximum, d_{exp} is the d-spacing calculated using XRD patterns in Fig. 1 and d_{hkl} is the d-spacing taken from JCPDS card nos. 72-2303 and 39-1346. Crystallite size (Fig. 2) increased as molar concentration was raised from 0.6mM to 1.4mM accompanied by decrease in dislocation density and strain. In case of sol-gel method, particle growth involves three steps including nucleation, coalescence of nuclei and subsequent growth of nanoparticles (Riaz et al. 2014a,b). With increase in molar concentration, colloidal particles become larger in number. Thus electrostatic collisions among the particles become high. This results in increase in electrostatic interactions among the particles. As a result of which, crystallite size increases. In addition, it can be seen that crystallite size is strongly affected by strain in thin films (Riaz and Naseem 2007).



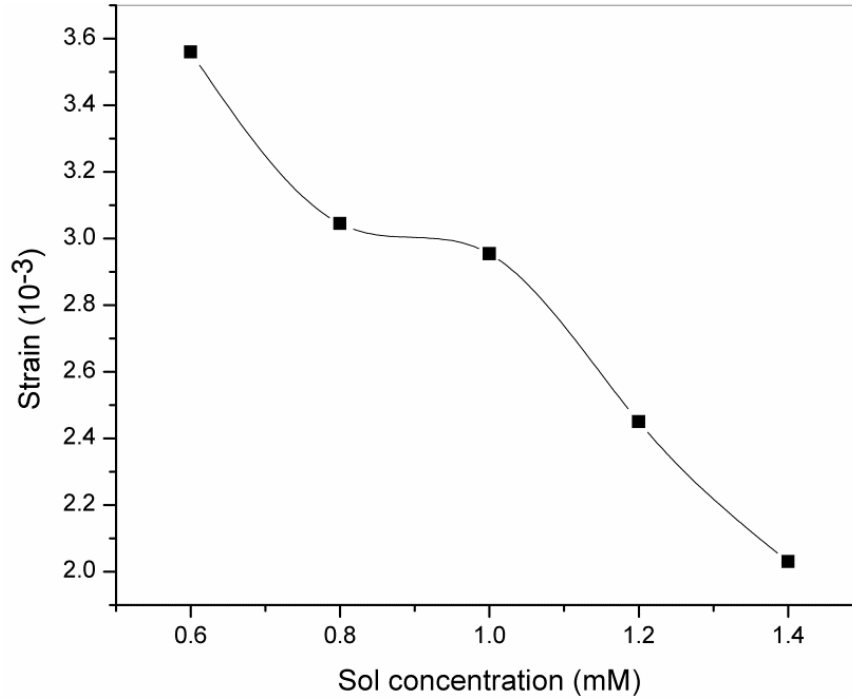


Fig. 2 Crystallite size, dislocation density and strain plotted as a function of sol concentration

Lattice parameters (a , c) and x-ray density (ρ , g/cm^3) (Cullity 1956) were determined using Eqs. 4-5.

$$\sin^2 \theta = \frac{\lambda^2}{4a^2} (h^2 + k^2 + l^2) \quad (4)$$

$$\rho = \frac{1.66042 \Sigma A}{V} \quad (5)$$

Where, ΣA is the sum of atomic weights in the unit cell and V is the volume of unit cell in \AA^3 . Lattice parameters and unit cell volume for iron oxide thin films are listed in table 1. Increase in lattice parameter and unit cell volume with increase in sol concentration is attributed to phase transition from $\gamma\text{-Fe}_2\text{O}_3$ to Fe_3O_4 .

Table 1 Lattice parameters and unit cell volume for iron oxide thin films

Sol concentration (mM)	Lattice parameter (\AA)	Unit cell volume (\AA^3)
0.6	8.352	582.6013
0.8	8.353	582.8106
1.0	8.359	584.0674
1.2	8.375	587.4277
1.4	8.390	590.5897

Fig. 3 shows magnetic hysteresis loops for iron oxide thin films. All the films demonstrate ferromagnetic behavior. Saturation magnetization (M_s) increased as molar concentration was decreased from 1.4mM to 0.8mM. This increase in saturation

magnetization is attributed to inclusion of $\gamma\text{-Fe}_2\text{O}_3$ phase in Fe_3O_4 . However, as sol concentration was further decreased to 0.6mM decrease in saturation magnetization is attributed to change in preferred orientation as observed in Fig. 1.

In case of magnetic materials, magnetization direction is strongly affected by crystallographic orientation of the films. Changes in preferred orientation, in thin films, dictate easy and hard axes of magnetization. In addition, domain structure, permeability along with magnetization process strongly depend on the film's preferred orientation (Riaz et al. 2013, 2014b, Akbar et al. 2014b). Further, Fe_3O_4 and $\gamma\text{-Fe}_2\text{O}_3$ have comparable structure with difference that because of the lack of Fe^{2+} cations in $\gamma\text{-Fe}_2\text{O}_3$ there are vacancies in the lattice. These vacancies lead to reduced magnetization (Fig. 4) as compared to that of Fe_3O_4 . But, in the present work, saturation magnetization increases with incorporation of $\gamma\text{-Fe}_2\text{O}_3$ in Fe_3O_4 . This increase in magnetization is accredited to outward diffusion of iron cations as was discussed in the XRD patterns.

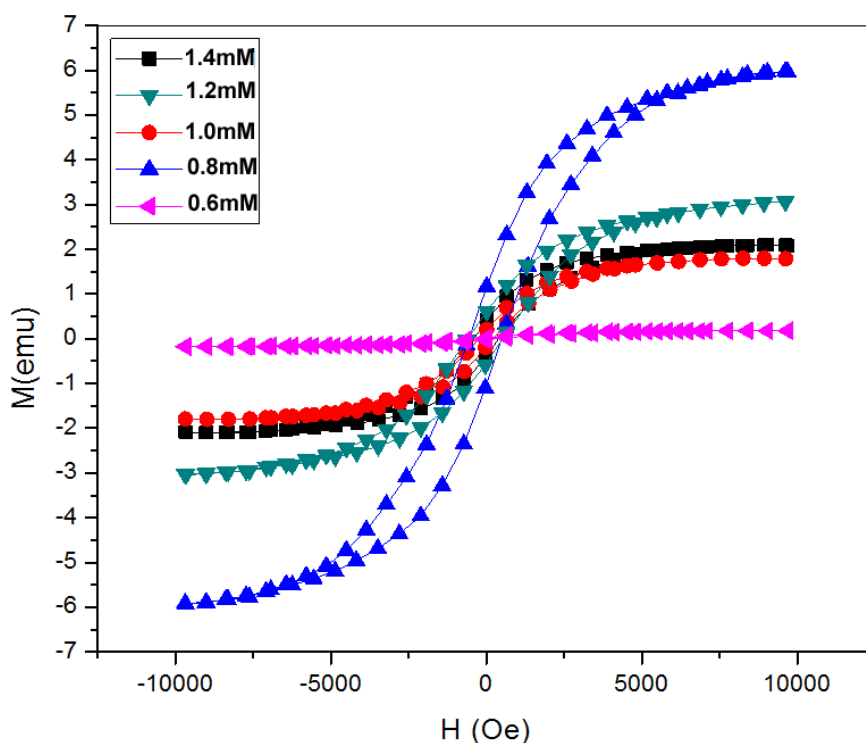


Fig. 3 M-H curves for iron oxide thin films

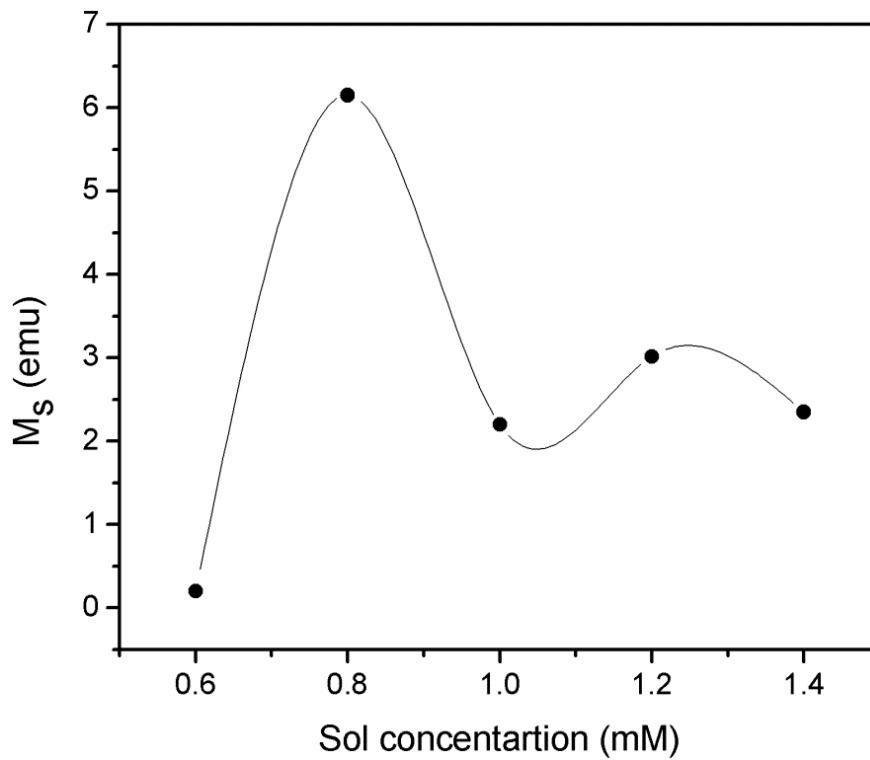


Fig. 4 Saturation magnetization (M_s) plotted as a function of sol concentration

Half metallic properties were studied using LDA and LDA+U. Partial and total density of states are plotted in Figs. 5(a) and (b) and Figs. 6 (a) and (b), respectively and investigated to observe magnetic nature and to confirm band gap of wüstite.

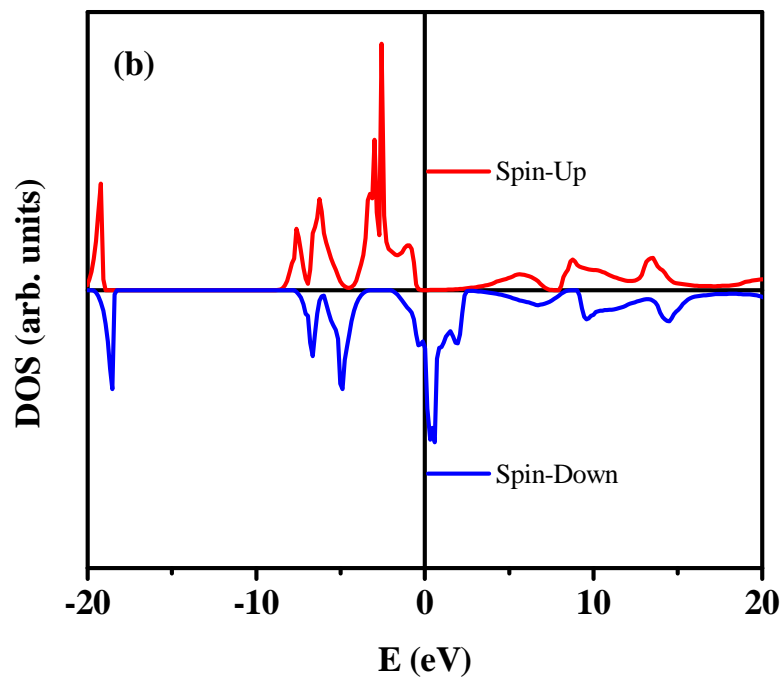
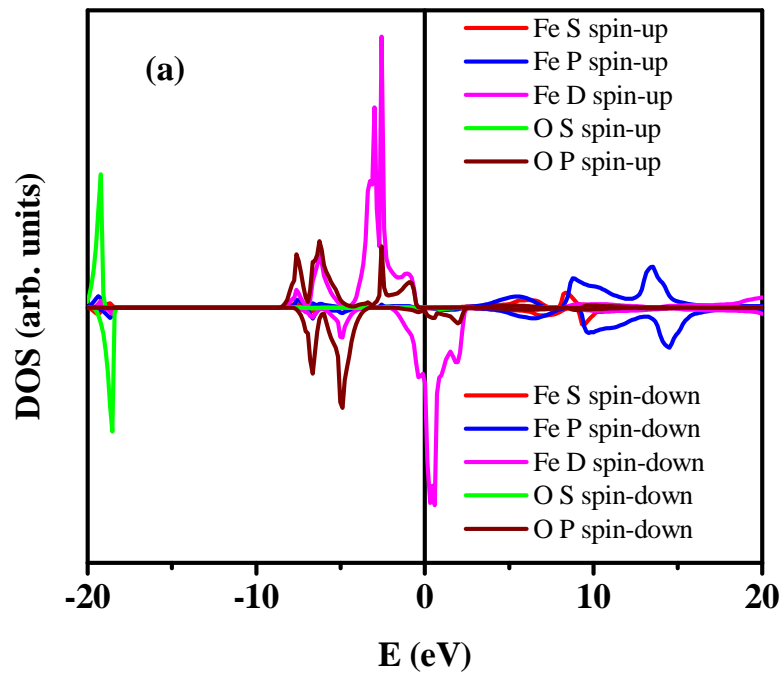


Fig. 5 a) Partial and b) Total DOS by LDA

Total and partial density of states is calculated by LDA+U. Fig. 6 (a) and (b) show partial and total density of states calculated by LDA+U.

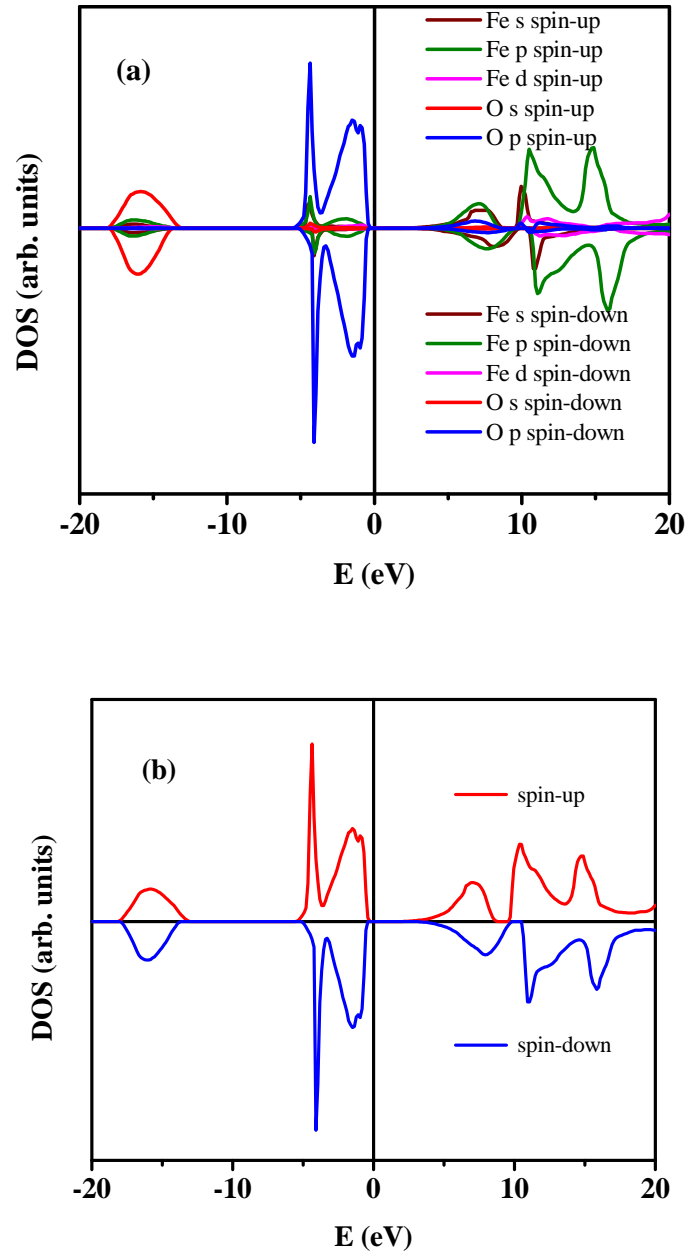


Fig. 6 a) partial and b) total DOS by LDA+U

Band gap values obtained at 0K by LDA and LDA+U are given in Table 2. In FeO, high magnetization configuration was obtained due to division of d electrons in majority spin and minority spin. Normally five d electrons occupy majority spin states and remaining one occupies the minority spin states (Himmetoglu et al. 2014). Antiferromagnetic behavior of wüstite was observed from Fig. 6 (a) and Fig. 6 (b),

which is in accordance to the experimentally obtained magnetic behavior of wüstite (Wdowik et al. 2015).

Table 2 Comparison of band gap values by LDA and LDA+U (U=0.6 eV)

Used approximation in ADF	Hubbard potential(eV)	Obtained band gap (eV) at 0K
LDA	0.0	0.00
LDA+U	0.6	2.08
Experimentally reported (Eom et al. 2015)		2.4

4. CONCLUSIONS

Iron oxide thin films were prepared using application oriented sol-gel and spin coating process. Sol's molar concentration was varied as 0.6mM-2.4mM. XRD patterns confirmed the formation of phase pure Fe_3O_4 at sol concentration 1.4mM with preferred orientation along (400) plane. Incorporation of γ - Fe_2O_3 phase was observed at low sol concentration of 0.8mM-1.2mM without change in preferred orientation. Change in preferred orientation to (321) plane took place at sol concentration 0.6mM. Saturation magnetization increased with decrease in sol concentration till 0.8mM. Due to change in preferred orientation reduction in magnetic properties was observed at low sol concentration 0.6mM. Half metallic behavior of Fe_3O_4 was observed using DFT. LDA+U with hubbard potential of 0.6 eV showed band gap value of 2.08 eV.

REFERENCES

- Akbar, A. Riaz, S. Ashraf, R. and Naseem, S. (2014a), "Magnetic and magnetization properties of Co-doped Fe_2O_3 thin films", *IEEE Trans. Magn.*, **50**, 2201204.
- Akbar, A. Riaz, S. Ashraf, R. and Naseem, S. (2015), "Magnetic and magnetization properties of iron oxide thin films by microwave assisted sol-gel route", *J. Sol-Gel Sci. Technol.*, **74**, 320-328.
- Akbar, A. Riaz, S. Bashir, M. and Naseem, S. (2014b), "Effect of Fe^{3+}/Fe^{2+} ratio on superparamagnetic behavior of spin coated iron oxide thin films," *IEEE Trans. Magn.*, **50**, 2200804.
- Alraddadi, S. Hines, W. Yilmaz, T. Gu, G.D. and Sinkovic, B. (2016), "Structural phase diagram for ultra-thin epitaxial $Fe_3O_4/MgO(0\ 0\ 1)$ films: Thickness and oxygen pressure dependence" *J. Phys.: Condens. Matter*, **28**, 115402.
- Asghar, M.H. Placido, F. and Naseem, S. (2006(a)), "Characterization of reactively evaporated TiO_2 thin films as high and medium index layers for optical applications" *Eur. Phys. J. - Appl. Phys.*, **35**, 177-184.
- Asghar, M.H. Placido, F. and Naseem, S. (2006(b)), "Characterization of Ta_2O_5 thin films prepared by reactive evaporation", *Eur. Phys. J. - Appl. Phys.*, **36**, 119-124.
- Barsoukov, E. and Macdonald, J.R. (2005), "Impedance spectroscopy theory: Experiment and applications", John Wiley & Sons, Inc., New Jersey.

- Bohra, M. Prasad, K.E. Bollina, R. Sahoo, S.C. and Kumar, N. (2016), "Characterizing the phase purity of nano crystalline Fe₃O₄ thin films using Verwey transition," *J. Magn. Magn. Mater.*, <http://dx.doi.org/10.1016/j.jmmm.2016.02.010>.
- Craik, D. J. (1975), "Magnetic Oxides", New York: Wiley.
- Cullity, B.D. (1956), "Elements of x-ray diffraction," Addison Wesley Publishing Company, USA.
- Gilks, D. Lari, L. Matsuzaki, K. Hosono, H. Susaki, T. and Lazarov, V.K. (2014), "Structural study of Fe₃O₄ (111) thin films with bulk like magnetic and magnetotransport behavior", *J. Appl. Phys.*, **115**, 17C107.
- Guan, X. Zhou, G. Xue, W. Quan, Z. and Xu, X. (2016), "The investigation of giant magnetic moment in ultrathin Fe₃O₄ films". *APL Mater.*, **4**, 036104.
- Hevroni, A. Bapna, M. Piotrowski, S. Majetich, S.A. and Markovich, G. (2016), "Tracking the Verwey transition in single magnetite nanocrystals by variable-temperature Scanning Tunneling Microscopy", *J. Phys. Chem. Lett.*, **7**, 1661–1666.
- Jolivet, J.P. and Tronc, E. (1988), "Interfacial electron transfer in colloidal spinel iron oxide: Conversion of Fe₃O₄- γ -Fe₂O₃ in aqueous medium", *J. Colloid Inter. Sci.*, **125**, 688-701.
- Kumar, N. Sharma, V. Parihar, U. Sachdeva, R. Padha, N. and Panchal, C.J. (2011), "Structure, optical and electrical characterization of tin selenide thin films deposited at room temperature using thermal evaporation method", *J. Nano- Electron. Phys.*, **3**, 117-126.
- Riaz, S. Akbar, A. and Naseem, S. (2013), "Structural, electrical and magnetic properties of iron oxide thin films", *Adv. Sci. Lett.*, **36**, 828-833.
- Riaz, S. Akbar, A. and Naseem, S. (2014a), "Ferromagnetic effects in Cr-Doped Fe₂O₃ thin films", *IEEE Trans. Magn.*, **50**, 2200704.
- Riaz, S. Ashraf, R. Akbar, A. and Naseem, S. (2014b), "Microwave assisted iron oxide nanoparticles—Structural and magnetic properties", *IEEE Trans. Magn.*, **50**, 2201504.